Bull. Mater. Sci. (2018) 41:19
https://doi.org/10.1007/s12034-017-1537-3

Elastic and thermodynamic properties of zirconium- and hafnium-doped Rh_3V intermetallic compounds: potential aerospace material

M MANJULA, M SUNDARESWARI* and E VISWANATHAN
Department of Physics, Sathyabama University, Chennai 600119, India
*Author for correspondence (sundare65@gmail.com)

MS received 24 February 2017; accepted 9 April 2017; published online 2 February 2018

Abstract. Structural, electronic, mechanical and thermodynamic properties of $Rh_3Zr_xV_{1-x}$ and $Rh_3Hf_xV_{1-x}$ ($x = 0$, 0.125, 0.25, 0.75, 0.875 and 1) combinations are investigated by means of first-principles calculations based on the density functional theory within the generalized gradient approximation. Here, Rh_3V is chosen as the parent binary compound and the doping elements are zirconium and hafnium with the above-mentioned concentrations. The calculated lattice parameters and elastic modulus of binary Rh_3Hf, Rh_3V and Rh_3Zr are in good agreement with the available experimental and other theoretical results. In this study, the following ternary materials viz., $Rh_3Zr_{0.75}V_{0.25}$, $Rh_3Hf_{0.25}V_{0.75}$ and $Rh_3Hf_{0.75}V_{0.25}$ are found to be brittle/more brittle than the parent binary compound Rh_3V, whereas the other ternary combinations, namely $Rh_3Zr_{0.125}V_{0.875}$, $Rh_3Zr_{0.25}V_{0.75}$, $Rh_3Zr_{0.875}V_{0.125}$, $Rh_3Hf_{0.125}V_{0.875}$ and $Rh_3Hf_{0.875}V_{0.125}$ are found to be more ductile than Rh_3V. The more brittle ternary combination, namely $Rh_3Hf_{0.75}V_{0.25}$ ($B = 229.32$ GPa) has the maximum Young's modulus, shear modulus and hardness values; whereas the more ductile ternary $Rh_3Zr_{0.25}V_{0.75}$ combination ($B = 243.54$ GPa) is found to have the least values of Young's modulus, shear modulus and hardness. The band structure, density of states histograms and charge density plots are drawn and discussed. Computed Debye temperature (θ_D), Grüneisen parameter (ζ) and melting temperature (T_m) of the parent binary compound Rh_3V, the more brittle $Rh_3Hf_{0.75}V_{0.25}$ combination and the more ductile $Rh_3Zr_{0.25}V_{0.75}$ combination are given by (895 K, 1.3491, 2788 K), (790 K, 1.2701, 2736 K) and (698 K, 1.7972, 2529 K), respectively.

Keywords. Electronic band structure; elastic properties; mechanical properties; ductility; Debye temperature.

1. Introduction

Refractory materials in the form of intermetallics are used in all major industries, such as electronics, aerospace, automotive, chemicals, mining, nuclear technology, metal processing and prosthetics. Generally, refractory metals refer to niobium, molybdenum, tantalum, tungsten, rhenium, titanium, vanadium, chromium, zirconium, hafnium, ruthenium, rhodium, osmium and iridium. Of these metals, ruthenium, rhodium, osmium and iridium are referred as platinum group refractory metals (along with platinum and palladium) as they resemble with platinum in their structural, physical and chemical properties. Further, they tend to occur together in the same mineral deposits. Platinum group metals (PGM) exhibit high density, high melting point, high electrical conductivity and low reactivity [1–6]. Due to their unique and desirable properties, they are used for high temperature structural applications, such as making cutting tools, aircraft gyroscope, aerospace engine components, nuclear reaction control rods and catalysts, etc. [3–12]. Experimental and band structure investigations on rhodium- and iridium-based intermetallics exist in the literature [3–22]. Chen *et al* [15] made the first effort to determine the elastic constants of Rh and Rh_3X compounds (X = V, Nb, Ta, Ti, Zr and Hf) and they have reported the decreasing order of brittleness as: $Rh_3V > Rh_3Ta > Rh_3Nb > Rh > Rh_3Zr > Rh_3Hf > Rh_3Ti$. From the literature survey [15,16], it is understood that rhodium with fifth group elements, such as V, Nb and Ta leads to more brittle materials, namely $Rh_3V > Rh_3Ta > Rh_3Nb$ than rhodium with fourth group elements, such as Zr, Hf and Ti [15,16] that resulted in $Rh_3Zr > Rh_3Hf > Rh_3Ti$. This motivated us to choose Rh_3V, the most brittle material as the parent material and to investigate on the ternary combinations, such as $Rh_3Zr_xV_{1-x}$ and $Rh_3Hf_xV_{1-x}$ ($x = 0$, 0.125, 0.25, 0.75, 0.875 and 1) by doping Rh_3V with fourth group elements, namely zirconium and hafnium.

2. Computational details

In our previous study [23], we have reported on the band structure calculations of Rh_3Ti doped with vanadium, niobium and tantalum. In the present study, structural, electronic, elastic, bonding and mechanical properties of $Rh_3Zr_{0.125}V_{0.875}$, $Rh_3Zr_{0.25}V_{0.75}$, $Rh_3Zr_{0.75}V_{0.25}$, $Rh_3Zr_{0.875}V_{0.125}$, $Rh_3Hf_{0.125}V_{0.875}$, $Rh_3Hf_{0.25}V_{0.75}$, $Rh_3Hf_{0.75}V_{0.25}$, $Rh_3Hf_{0.875}V_{0.125}$,

Rh_3Hf, Rh_3Zr and Rh_3V are studied by first principles band structure calculations using the density functional theory (DFT) within the local density approximation (LDA) and the generalized gradient approximation (GGA). The stability, bonding mechanism, ductile/brittle behaviour and thermal properties of these alloys are analysed and reported. In addition, Debye temperature, Grüneisen parameter and melting temperature values are calculated for these alloy combinations.

In the present work, the full potential linearized augmented plane wave method implemented in the WIEN2k code [24] is employed. Generalized gradient approximation (GGA) [25] with the Perdew–Burke–Ernzerhof (PBE) [26] and LDA [27] with the Perdew and Zunger [28] are considered in the present study. The integration in the Brillion zone was done by using Monkhorst Pack $14 \times 14 \times 14$ k-points for Rh_3V and $10 \times 10 \times 10$ k-points for $Rh_3(Zr,Hf)_xV_{1-x}$ compositions. To achieve convergence, we have chosen $R_{MT} * K_{max} = 7$, $l_{max} = 10$ and $G_{max} = 12$ for the present calculation. The total energies and charges are converged below 10^{-4} eV and 10^{-3} mRy, respectively. Calculations for parent Rh_3V and its ternary combinations such as $Rh_3(Zr,Hf)_xV_{1-x}$ ($x = 0.125$, 0.25, 0.75 and 0.875) are carried out as in our previous study [23].

The elastic constants (C_{11}, C_{12} and C_{44}), Young's modulus, shear modulus, Cauchy pressure, G/B ratio, Poisson's ratio, anisotropy energy and hardness are calculated for $Rh_3(Zr,Hf)_xV_{1-x}$ ($x = 0$, 0.125, 0.25, 0.75, 0.875 and 1) compounds with the optimized lattice constant obtained with GGA exchange correlation and are listed in table 1.

3. Results and discussion

3.1 *Structural properties*

Rh_3V crystallizes in Cu_3Au type structure (space group *Pm3m* and space group number 221). The unit cell contains three rhodium atoms and one vanadium atom, where rhodium and vanadium atoms are located at (0, 0.5, 0.5) and (0, 0, 0) positions, respectively. The total energy per atom as a function of volume for each of the $Rh_3(Zr,Hf)_xV_{1-x}$ ($x = 0, 0.125$, 0.25, 0.75, 0.875 and 1) compounds are calculated using GGA and LDA and the curves were fitted to the Birch–Murnaghan equation of states [29] to compute the ground state properties. The volume optimization curves (both LDA and GGA) for binary Rh_3V, Rh_3Zr and Rh_3Hf compounds are shown in figure 1a–c and that for the ternary combinations with GGA are shown in figure 2a–h. The calculated ground state properties such as lattice parameters and bulk modulus for cubic $Rh_3(Zr,Hf)_xV_{1-x}$ ($x = 0$, 0.125, 0.25, 0.75, 0.875 and 1) compounds are listed in table 1. Optimized lattice constants of binary compounds agree very well with the available experimental and theoretical values.

3.2 *Electronic properties*

3.2a *Band structures*: The self-consistent band structures of parent Rh_3V compound are shown in figure 3a–e. From figure 3c and e, where fat bands are drawn for Rh-d and V-d, it is understood that the states around the Fermi level in Rh_3V are significantly due to Rh-d and V-d states; further there is also a feeble contribution from Rh-p and V-p states as shown by the respective fat bands in figure 3b and d. Comparing figure 3a with figure 3b–e, one could state that in Rh_3V, above the Fermi level in the direction R–Λ, there is hybridization between p- and d-states of rhodium and vanadium around 0.6 eV. Band structures of each of $Rh_3V_{1-x}(Zr,Hf)_x$ ($x = 0.125$, 0.25, 0.75 and 0.875) compounds are plotted and are presented in figures 4a–d and 5a–d, respectively, for zirconium- and hafnium-doped ternary combinations. From the band structures of figure 4a–d, one can say that the bands at the Fermi level originate from the interaction of Rh-d and hybridized d-states of V and Zr. The s- and p-states of Rh, V and Zr elements do not contribute much at the Fermi energy level. From figure 4a, which is drawn for $Rh_3Zr_{0.125}V_{0.875}$, one can observe that the bands around −0.6 eV are due to Rh-d states and hybridized V-d and Zr-d states and they cross the Fermi level at Λ along R–Λ direction; whereas the same bands are found to lie around 0.1 eV, hence, shifted just above the Fermi level for $Rh_3Zr_{0.875}V_{0.125}$ combination as shown in figure 4d. Similarly, in figure 4b, which is drawn for $Rh_3Zr_{0.25}V_{0.75}$, one can note that the bands at −0.4 eV are due to Rh-d and hybridized V-d and Zr-d like electrons which cross the Fermi level at Λ along P–Λ direction; whereas the same bands are shifted to the states around 0.05 eV that lie above the Fermi level in $Rh_3Zr_{0.75}V_{0.25}$ as shown in figure 4c. The band profile of $Rh_3Hf_xV_{1-x}$ ($x = 0.125$, 0.25, 0.75 and 0.875) combinations (figure 5a–d) are very similar to that of $Rh_3Zr_xV_{1-x}$ ($x = 0.125$, 0.25, 0.75 and 0.875) combinations (figure 4a–d). The non-vanishing bands at the Fermi energy level depict the metallic nature of the materials under the present study.

3.2b *Density of states*: The total and partial density of states of $Rh_3(Zr,Hf)_xV_{1-x}$ ($x = 0.125$, 0.25, 0.75 and 0.875) compounds are plotted and are shown in figures 6a–d and 7a–d. Here, the peaks that lie below the Fermi level are due to Rh-d like electrons, and that lie above the Fermi level are due to V-d like and Zr-d (or Hf-d) like electrons for $Rh_3V_{(1-x)}Zr_x$ and $Rh_3V_{(1-x)}Hf_x$ combinations, respectively. Comparing the figures 6a–d and 7a–d, one could observe the presence of deep valley at the close proximity of Fermi energy level, the so called pseudogap only in the following combinations, namely $Rh_3Zr_{0.75}V_{0.25}$ (figure 6c), $Rh_3Hf_{0.75}V_{0.25}$ (figure 7a) and $Rh_3Hf_{0.25}V_{0.75}$ (figure 7b) at 8, 8, 10 eV per state, respectively. The presence of such pseudogap reflects the strength of covalent bonding of the given material. Hence, predominant covalent nature could be seen in $Rh_3Zr_{0.75}V_{0.25}$, $Rh_3Hf_{0.75}V_{0.25}$ and $Rh_3Hf_{0.25}V_{0.75}$. The same is witnessed in the charge density plots and also while analysing the ductile/brittle nature in the following section.

Table 1. Calculated ground state and elastic properties of $Rh_3(Zr,Hf)_xV_{1-x}$ ($x = 0$, 0.125, 0.25, 0.75, 0.875 and 1) compounds.

	Parameters											
Alloy combinations	Lattice constant (a.u.)	C_{11} (GPa)	C_{12} (GPa)	C_{44} (GPa)	$(C_{12}-C_{44})$ (GPa)	B (GPa)	G (GPa)	E (GPa)	G/B	ν	A	H_V (GPa)
Rh_3V	$a_{exp.} = 7.17391$ 7.1716[a] 7.154[b] $a_{cal.} = 7.2014$ (GGA) 7.056 3(LDA) 7.2434[a] 7.086[b]	429.02 410.08[c]	164.33 181.41[c]	223.68 199.04[c]	−59.35	258.55 257.63[c]	181.21 159.35[c]	438.71 396.34[c]	0.71	0.21 0.24[c]	1.43	34.98
$Rh_3Zr_{0.125}V_{0.875}$	$a_{opt.} = 7.2396$ (GGA) 7.0926 (LDA)	381.28	186.43	177.61	8.82	251.38	139.58	353.33	0.55	0.27	1.42	21.79
$Rh_3Zr_{0.25}V_{0.75}$	$a_{opt.} = 7.2759$ (GGA) 7.1278 (LDA)	346.05	192.29	139.67	52.62	243.54	109.91	286.63	0.45	0.30	1.36	14.37
$Rh_3Zr_{0.75}V_{0.25}$	$a_{opt.} = 7.4189$ (GGA) 7.2678 (LDA)	361.05	158.24	186.38	−28.14	225.84	145.99	360.33	0.64	0.23	1.47	25.88
$Rh_3Zr_{0.875}V_{0.125}$	$a_{opt.} = 7.4451$ (GGA) 7.3056 (LDA)	347.28	161.69	150.84	10.85	223.55	124.14	314.25	0.56	0.27	1.33	19.38
Rh_3Zr	$a_{opt.} = 7.4773$ (GGA) 7.3428 (LDA) 7.4948[a] 7.356[b]	343.19 351.8[d]	159.22 196[d]	101.12 77.8[d]	58.1	220.54 248[d]	97.36 77.8[d]	254.61 211.4[d]	0.44	0.31 0.35[d]	1.05 0.99[d]	12.48
$Rh_3Hf_{0.125}V_{0.875}$	$a_{opt.} = 7.2376$ (GGA) 7.0895 (LDA)	378.16	179.18	193.35	−14.17	245.51	148.09	369.89	0.60	0.25	1.49	24.79
$Rh_3Hf_{0.25}V_{0.75}$	$a_{opt.} = 7.2699$ (GGA) 7.1174 (LDA)	366.82	162.03	192.56	−30.53	230.29	149.45	370.48	0.65	0.23	1.49	26.87
$Rh_3Hf_{0.75}V_{0.25}$	$a_{opt.} = 7.3953$ (GGA) 7.2455 (LDA)	420.29	133.84	183.80	−49.96	229.32	166.33	401.84	0.73	0.21	1.19	32.38
$Rh_3Hf_{0.875}V_{0.125}$	$a_{opt.} = 7.4146$ (GGA) 7.2748 (LDA)	355.45	169.47	164.68	4.79	215.68	130.93	326.69	0.60	0.25	1.40	22.03
Rh_3Hf	$a_{opt.} = 7.4815$ (GGA) 7.2869 (LDA) 7.4645[a] 7.346[b]	361.43 296[a]	133.81 158[a]	72.77 140[a]	61.04	209.69 204[a]	87.11 105[a]	229.55 270[a]	0.42 0.52[a]	0.32 0.28[a]	0.77	10.59

[a]Ref. [15], [b]ref. [17], [c]ref. [22], [d]ref. [21].

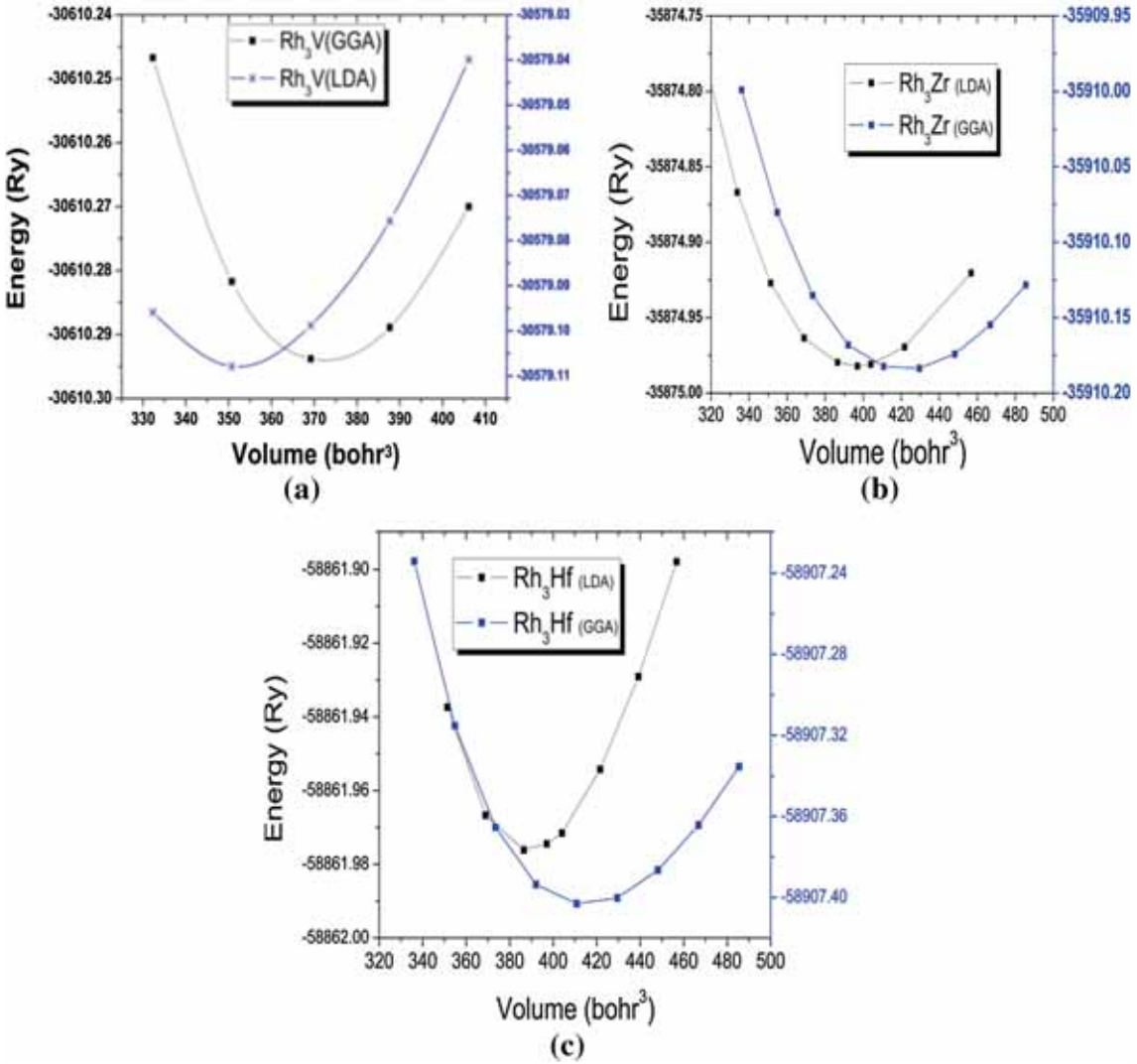

Figure 1. Energy *vs*. volume of (**a**) Rh_3V, (**b**) Rh_3Zr and (**c**) Rh_3Hf.

3.3 *Elastic properties*

There are three independent elastic constants for cubic structure namely C_{11}, C_{12} and C_{44} and these values for the present system are listed in table 1. From this table, one could find that the mechanical stability conditions for cubic crystals, given by $C_{11}-C_{12} > 0$, $C_{11} > 0$, $C_{44} > 0$, $C_{11} + 2C_{12} > 0$ [30] are satisfied for the compounds under present study. Using elastic constants, the other parameters such as bulk modulus, shear modulus, Young's modulus, Cauchy pressure, G/B ratio, Poisson's ratio (ν), anisotropy factor (A) and hardness (H_v) are calculated and are presented in table 1.

3.3a *Ductile/brittle analysis*: In metals and compounds, the angular character of atomic bonding is described by using the Cauchy pressure [31]. It is negative for non-metallic with directional bonding materials (brittle) and positive for metallic characteristic materials (ductile). In the present study, among the zirconium-doped ternary combinations, the $Rh_3Zr_{0.75}V_{0.25}$ (−28.14 GPa) material has negative Cauchy pressure indicating the most brittle combination and the other compounds, namely $Rh_3Zr_{0.125}V_{0.875}$ (8.82 GPa), $Rh_3Zr_{0.25}V_{0.75}$ (52.62 GPa) and $Rh_3Zr_{0.875}V_{0.125}$ (10.85 GPa) combinations are found to have positive Cauchy pressure indicating their ductile nature (figure 8a). Similarly, in the case of hafnium-doped ternary combinations, the $Rh_3Hf_{0.75}V_{0.25}$ (−44.97 GPa) has the lowest Cauchy pressure, hence, the most brittle and the $Rh_3Hf_{0.875}V_{0.125}$ (4.79 GPa) combination has the highest value of Cauchy pressure, indicating the most ductile nature among hafnium-doped ternary combinations. The remaining hafnium-doped ternary combination, namely $Rh_3Hf_{0.125}V_{0.875}$ and $Rh_3Hf_{0.25}V_{0.75}$ have Cauchy pressure values of −14.18 and −32.53 GPa, respectively, and hence, they are identified as brittle materials (figure 8a). However, compared to the parent binary material, namely Rh_3V, the newly predicted ternary compounds (refer table 1

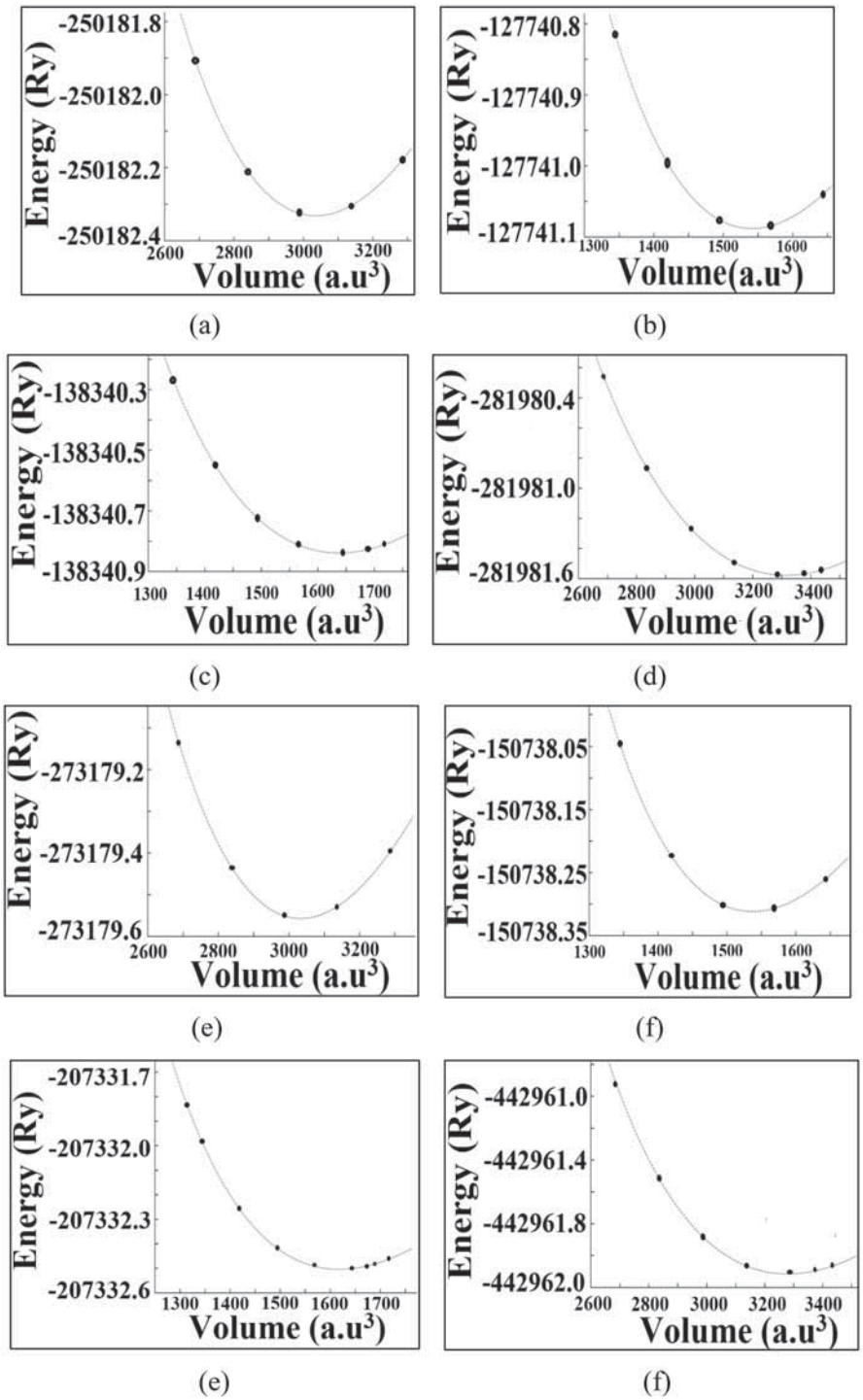

Figure 2. Total energy as a function of volume (**a**) $Rh_3Zr_{0.125}V_{0.875}$, (**b**) $Rh_3Zr_{0.25}V_{0.75}$, (**c**) $Rh_3Zr_{0.75}V_{0.25}$, (**d**) $Rh_3Zr_{0.875}V_{0.125}$, (**e**) $Rh_3Hf_{0.125}V_{0.875}$, (**f**) $Rh_3Hf_{0.25}V_{0.75}$, (**g**) $Rh_3Hf_{0.75}V_{0.25}$ and (**h**) $Rh_3Hf_{0.875}V_{0.125}$.

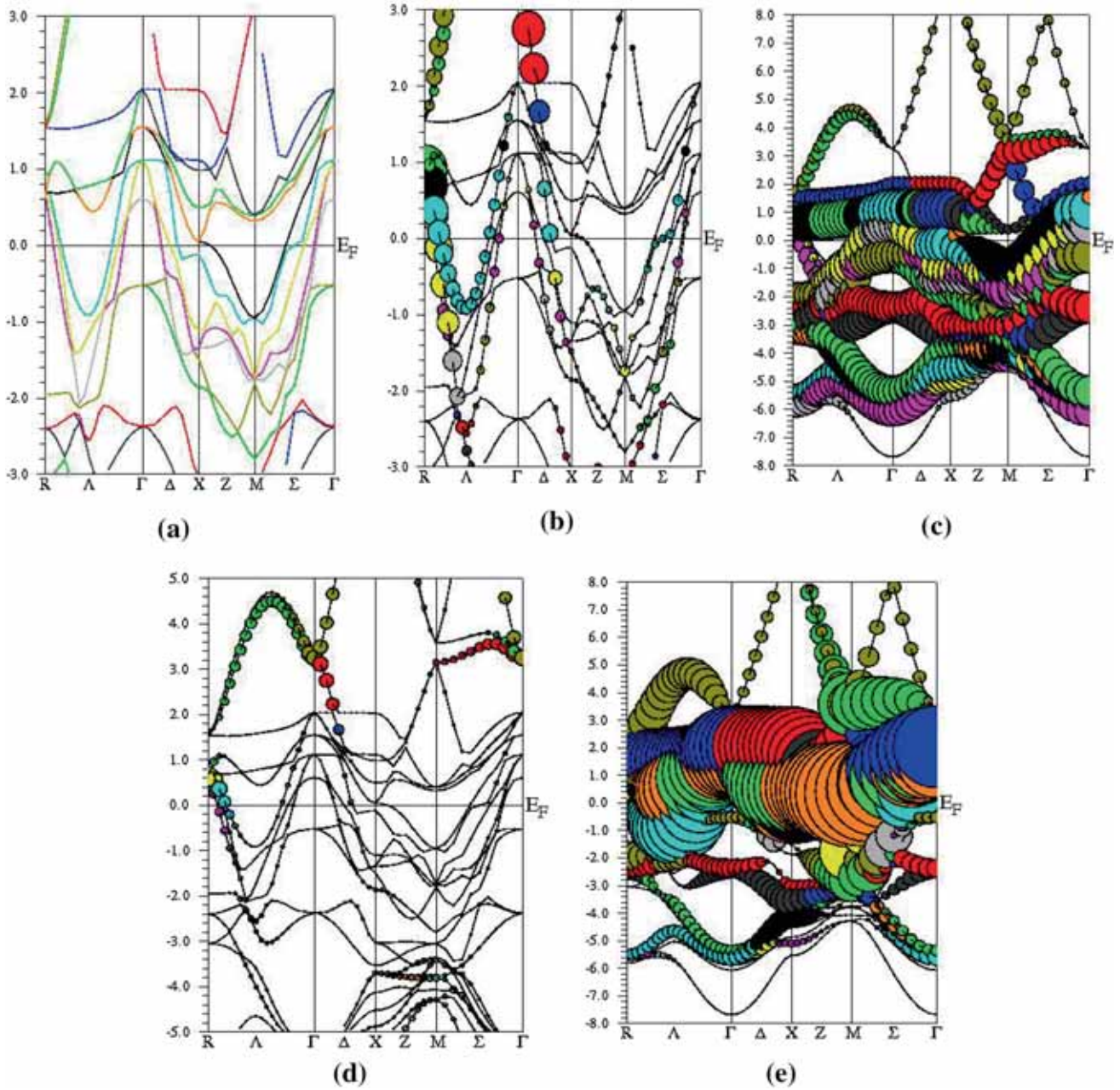

Figure 3. Band structure of (**a**) Rh_3V and fat band of (**b**) Rh-p, (**c**) Rh-d, (**d**) V-p and (**e**) V-d states of Rh_3V.

and figure 8a), namely $Rh_3Zr_{0.125}V_{0.875}$, $Rh_3Zr_{0.25}V_{0.75}$, $Rh_3Zr_{0.875}V_{0.125}$, $Rh_3Hf_{0.125}V_{0.875}$ and $Rh_3Hf_{0.875}V_{0.125}$ are found to be more ductile (more positive Cauchy pressure values) and $Rh_3Zr_{0.75}V_{0.25}$, $Rh_3Hf_{0.25}V_{0.75}$ and $Rh_3Hf_{0.75}V_{0.25}$ are identified as more brittle (more negative Cauchy pressure values).

The ratio of shear modulus to bulk modulus (G/B), introduced by Pugh [32] is used to predict the brittle/ductile behaviour of the given material. Out of the four zirconium-doped ternary $Rh_3Zr_xV_{1-x}$ ($x = 0.125$, 0.25, 0.75 and 0.875) combinations, for $Rh_3Zr_{0.125}V_{0.875}$ ($G/B = 0.55$), $Rh_3Zr_{0.25}V_{0.75}$ ($G/B = 0.45$) and $Rh_3Zr_{0.875}V_{0.125}$ ($G/B = 0.56$) combination, the value of G/B is found to be less than the critical value of 0.57 making them ductile. Similarly, when we consider hafnium-doped ternary combinations, one could find the value of G/B is greater than 0.57 for all the $Rh_3Hf_xV_{1-x}$ ($x = 0.125$, 0.25, 0.75 and 0.875) materials, making them brittle. When we compare the G/B ratio of the present eight ternary combinations with that of the parent Rh_3V ($G/B = 0.63$), the following compounds (refer table 1 and figure 8b), namely $Rh_3Zr_{0.125}V_{0.875}$, $Rh_3Zr_{0.25}V_{0.75}$, $Rh_3Zr_{0.875}V_{0.125}$,

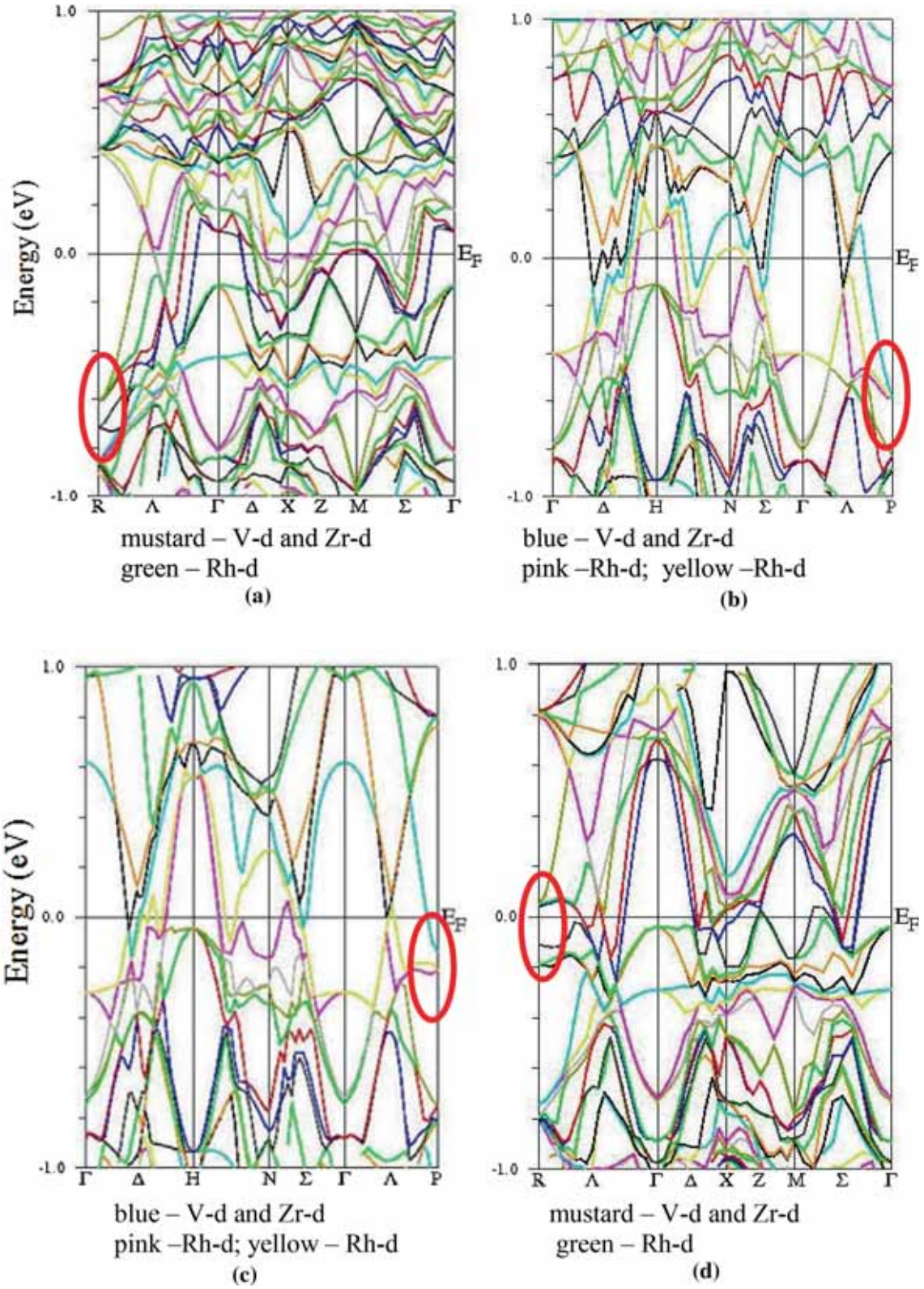

Figure 4. Band structure of (**a**) $Rh_3Zr_{0.125}V_{0.875}$, (**b**) $Rh_3Zr_{0.25}V_{0.75}$, (**c**) $Rh_3Zr_{0.75}V_{0.25}$ and (**d**) $Rh_3Zr_{0.875}V_{0.125}$.

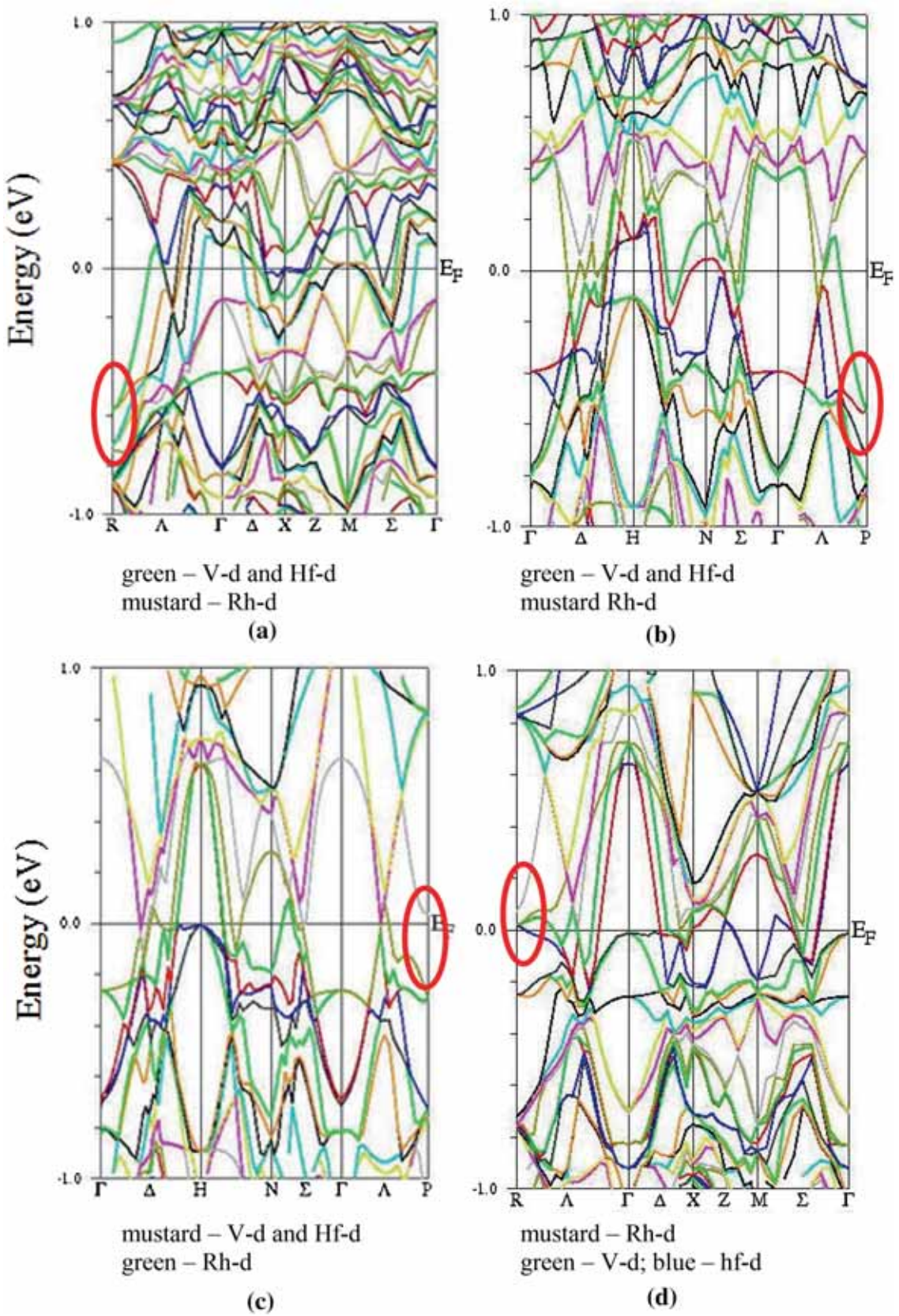

Figure 5. Band structure of (**a**) $Rh_3Hf_{0.125}V_{0.875}$, (**b**) $Rh_3Hf_{0.25}V_{0.75}$, (**c**) $Rh_3Hf_{0.75}V_{0.25}$ and (**d**) $Rh_3Hf_{0.875}V_{0.125}$.

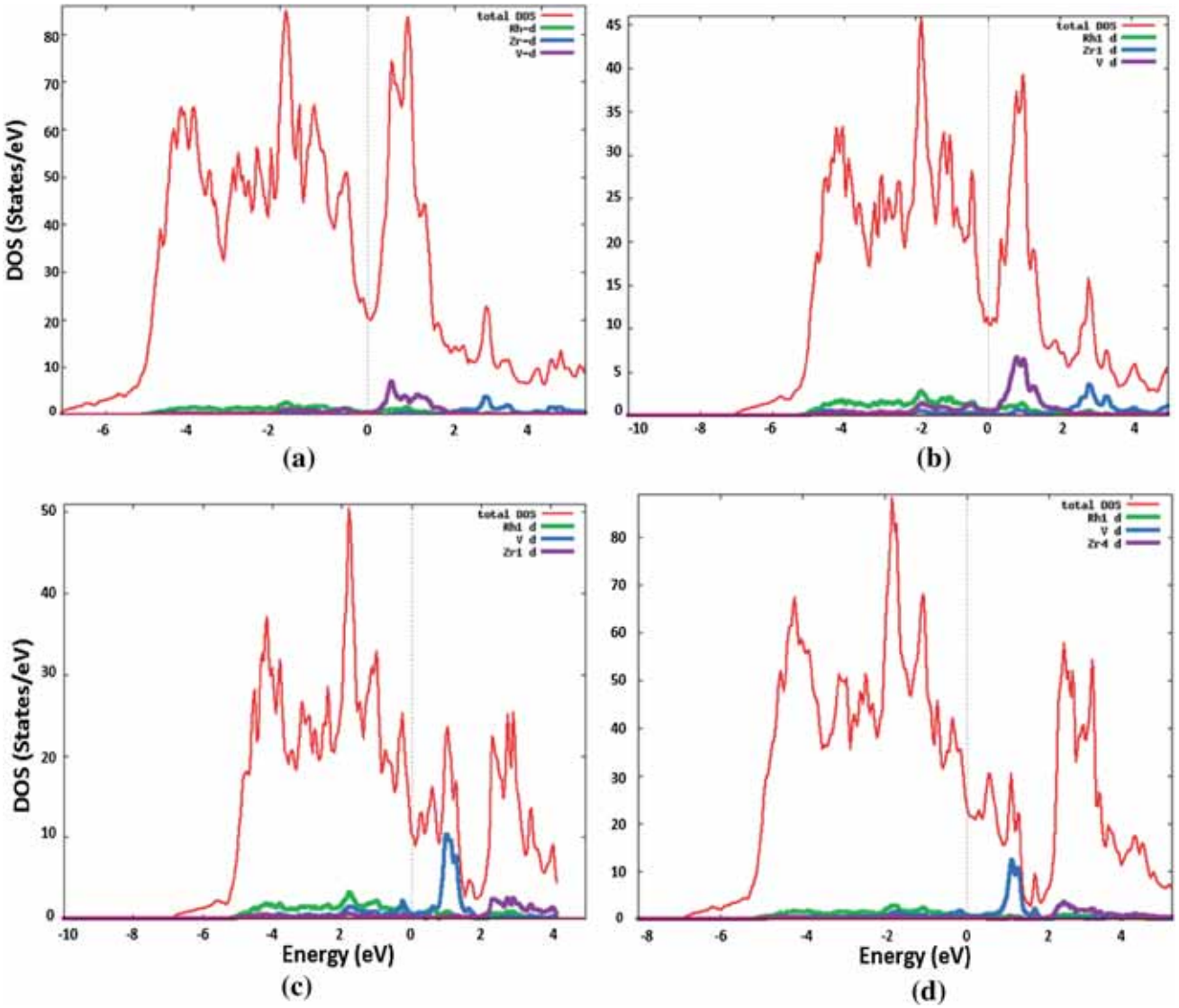

Figure 6. Total and partial density of states of (**a**) $Rh_3Zr_{0.125}V_{0.875}$, (**b**) $Rh_3Zr_{0.25}V_{0.75}$, (**c**) $Rh_3Zr_{0.75}V_{0.25}$ and (**d**) $Rh_3Zr_{0.875}V_{0.125}$.

$Rh_3Hf_{0.125}V_{0.875}$, $Rh_3Hf_{0.875}V_{0.125}$ are found to be more ductile (as their G/B values are <0.63) and $Rh_3Zr_{0.75}V_{0.25}$, $Rh_3Hf_{0.25}V_{0.75}$ and $Rh_3Hf_{0.75}V_{0.25}$ are identified as more brittle (as their G/B values are >0.63).

The other parameter that is used to predict brittle/ductile behaviour of metals and metallic compounds is Poisson's ratio [33]. From table 1, it can be noticed that the ν-values are <0.3 (or 0.25) for $Rh_3Hf_{0.25}V_{0.75}$, $Rh_3Hf_{0.75}V_{0.25}$ and $Rh_3Zr_{0.75}V_{0.25}$ combinations making them brittle; and for $Rh_3Hf_{0.125}V_{0.875}$, $Rh_3Hf_{0.875}V_{0.125}$, $Rh_3Zr_{0.125}V_{0.875}$, $Rh_3Zr_{0.875}V_{0.125}$ and $Rh_3Zr_{0.25}V_{0.75}$ combinations, the Poisson's ratio values are found to be >0.3 (or 0.25), making them ductile (figure 8c).

Based on the above analysis, it can be concluded that out of eight newly predicted $Rh_3(Zr,Hf)_xV_{1-x}$ ($x = 0.125$, 0.25, 0.75 and 0.875) materials, $Rh_3Zr_{0.125}V_{0.875}$, $Rh_3Zr_{0.25}V_{0.75}$, $Rh_3Zr_{0.875}V_{0.125}$, $Rh_3Hf_{0.125}V_{0.875}$ and $Rh_3Hf_{0.875}V_{0.125}$ combinations are identified as more ductile than the parent binary Rh_3V ($\nu = 0.24$) compound and the remaining three $Rh_3Zr_{0.75}V_{0.25}$, $Rh_3Hf_{0.25}V_{0.75}$ and $Rh_3Hf_{0.75}V_{0.25}$ combinations are identified as more brittle than the parent binary Rh_3V compound.

The above results can further be assessed by the charge density plots shown in figures 9a–d and 10a–d for $Rh_3(Zr,Hf)_xV_{1-x}$ ($x = 0.125$, 0.25, 0.75 and 0.875) combinations, respectively. Here, the charge density contours are also drawn for the binary compounds, namely Rh_3V, Rh_3Zr and Rh_3Hf and are presented in figure 11a–c. Generally, uniform distribution of directional charge density contours enclosing any two atoms indicates the presence of strong covalent nature between the two atoms. In figure 11a, one can find such directional contours (blue line) that enclose

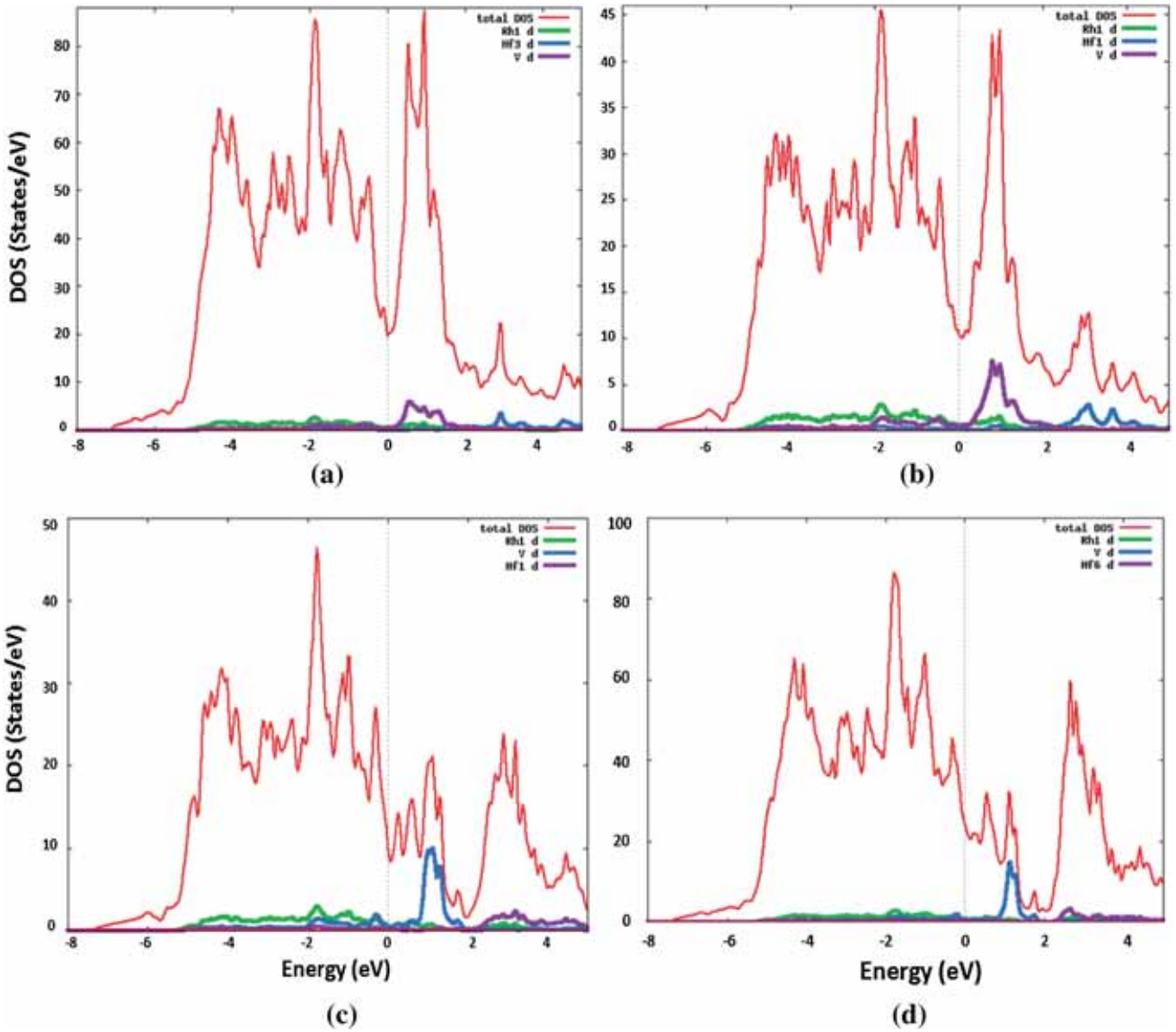

Figure 7. Total and partial density of states of (**a**) $Rh_3Hf_{0.125}V_{0.875}$, (**b**) $Rh_3Hf_{0.25}V_{0.75}$, (**c**) $Rh_3Hf_{0.75}V_{0.25}$ and (**d**) $Rh_3Hf_{0.875}V_{0.125}$.

V–Rh–V, confirming the strong covalent nature of Rh_3V. Whereas in figure 11b and c, no such directional contours are seen, instead one could find spherical contours around each of rhodium, zirconium and hafnium atoms in their respective binary compounds, indicating the metallic bonding nature of Rh_3Zr and Rh_3Hf. Considering figure 9a–d, one can find directional electron density contours enclosing V–Rh–Zr–Rh atoms in $Rh_3Zr_{0.75}V_{0.25}$ (figure 9c) that ensures the covalent nature, whereas such directional contours are absent in $Rh_3Zr_{0.125}V_{0.875}$, $Rh_3Zr_{0.25}V_{0.75}$ and $Rh_3Zr_{0.875}V_{0.125}$ compounds (figure 9a, b and d), hence, they are not covalent. Considering figure 10a–d, strong covalent nature (strong directional character) is seen in $Rh_3Hf_{0.25}V_{0.75}$ (figure 10b) and $Rh_3Hf_{0.75}V_{0.25}$ (figure 10c) combinations, whereas in $Rh_3Hf_{0.125}V_{0.875,}$ one could find weak covalent nature as there exist weak directional contours. In $Rh_3Hf_{0.875}V_{0.125}$ (figure 10d) combination, such directionality is absent, hence, they are not covalent.

Bulk modulus is correlated with binding energy or cohesive energy of atoms, since it is a measure of average atomic bond strength. From table 1, the descending trend of bulk modulus can be shown as $Rh_3V-Rh_3Zr_{0.125}V_{0.875}-Rh_3Zr_{0.25}V_{0.75}-Rh_3Zr_{0.75}V_{0.25}-Rh_3Zr_{0.875}V_{0.125}-Rh_3Zr$ for $Rh_3Zr_xV_{1-x}$ (x = 0.125, 0.25, 0.75 and 0.875) combinations; and for $Rh_3Hf_xV_{1-x}$ (x = 0, 0.125, 0.25, 0.75, 0.875 and 1) combinations, it follows the order as $Rh_3V-Rh_3Hf_{0.125}V_{0.875}-Rh_3Hf_{0.25}V_{0.75}-Rh_3Hf_{0.75}V_{0.25}-Rh_3Hf_{0.875}V_{0.125}-Rh_3Hf$.

Young's modulus (E) is one of the important quantities for technological and engineering applications. The material is stiffer for the larger value of E and the stiffer solids have covalent bonds [34,35]. From table 1, the stiffness of the $Rh_3Zr_xV_{1-x}$ (x = 0, 0.125, 0.25, 0.75, 0.875

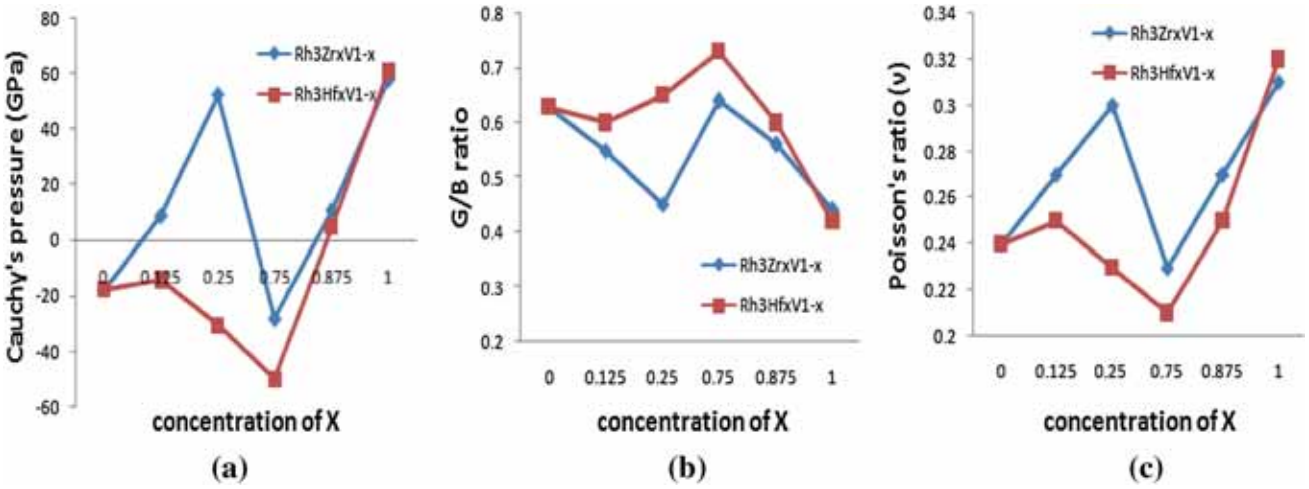

Figure 8. (**a–c**) Cauchy pressure, *G/B* ratio and Poisson's ratio *vs*. concentration of $Rh_3Zr_xV_{1-x}$ and $Rh_3Hf_xV_{1-x}$.

and 1) combinations decrease in the following order as: $Rh_3V-Rh_3Zr_{0.75}V_{0.25}-Rh_3Zr_{0.125}V_{0.875}-Rh_3Zr_{0.875}V_{0.125}-Rh_3Zr_{0.25}V_{0.75}-Rh_3Zr$; and for $Rh_3Hf_xV_{1-x}$ ($x = 0.125$, 0.25, 0.75 and 0.875) combinations, it follows the order as: $Rh_3Hf_{0.75}V_{0.25}-Rh_3V-Rh_3Hf_{0.25}V_{0.75}-Rh_3Hf_{0.125}V_{0.875}-Rh_3Hf_{0.875}V_{0.125}-Rh_3Hf$.

Shear modulus shows a monotonic variation with hardness [36,37] and this parameter is a better indication of the strength of the solid. Shear modulus (G) also follows (table 1) the same trend of Young's modulus in both $Rh_3Zr_xV_{1-x}$ and $Rh_3Hf_xV_{1-x}$ ($x = 0.125$, 0.25, 0.75 and 0.875) combinations. The $Rh_3Zr_{0.25}V_{0.75}$ (286.63 and 109.91 GPa) having the lowest and $Rh_3Zr_{0.75}V_{0.25}$ (360.33 and 145.99 GPa) with the highest E and G values among $Rh_3Zr_xV_{1-x}$ ($x = 0.125$, 0.25, 0.75 and 0.875) combinations; whereas as in $Rh_3Hf_xV_{1-x}$ ($x = 0.125, 0.25, 0.75$ and 0.875) combinations, $Rh_3Hf_{0.875}V_{0.125}$ (326.69 and 130.93 GPa) has the lowest E and G values and $Rh_3Hf_{0.75}V_{0.25}$ (418.57 and 175.02 GPa) has the highest E and G values, respectively.

The variations of bulk, Young's and shear moduli with concentrations of zirconium and hafnium in Rh_3V are drawn and shown in figure 12a and b, where one could see the highest G and E values in $Rh_3Zr_{0.75}V_{0.25}$ (360.33 and 145.99 GPa) and $Rh_3Hf_{0.75}V_{0.25}$ (418.57 and 175.02 GPa) combinations. The reason for the highest values in these two combinations is well explained in sections 3.2b and 3.3a.

The Vicker's microhardness (H_v) values are calculated for $Rh_3Zr_xV_{1-x}$ and $Rh_3Hf_xV_{1-x}$ ($x = 0$, 0.125, 0.25, 0.75, 0.875 and 1) combinations using the formula given in ref. [38]. Elastic constant C_{44} indirectly governs the indentation hardness. Hence, larger C_{44} represents the strong ability of resisting the monoclinic shear distortion. From table 1, one could notice that the decreasing trend of hardness for $Rh_3Zr_xV_{1-x}$ ($x = 0$, 0.125, 0.25, 0.75, 0.875 and 1) combinations follows the order as: $Rh_3V-Rh_3Zr_{0.75}V_{0.25}-Rh_3Zr_{0.125}V_{0.875}-Rh_3Zr_{0.875}V_{0.125}-Rh_3Zr_{0.25}V_{0.75}-Rh_3Zr$; and for $Rh_3Hf_xV_{1-x}$ ($x = 0.125$, 0.25, 0.75 and 0.875) combinations it follows the order as: $Rh_3Hf_{0.75}V_{0.25}-Rh_3V-Rh_3Hf_{0.25}V_{0.75}-Rh_3Hf_{0.125}V_{0.875}-Rh_3Hf_{0.875}V_{0.125}-Rh_3Hf$. The same trend is observed in Young's and shear moduli also.

The anisotropy factor (A) [39] is an indicator of the degree of anisotropy in the solid materials. It takes the value of 1 in complete isotropic material. If the value of A is smaller or greater than unity, it is a measure of the degree of elastic anisotropy. The present newly predicted materials have $A > 1$ (table 1), hence, the materials exhibit anisotropic nature.

3.4 *Debye temperature, Grüneisen parameter and melting temperature*

The sound velocities for longitudinal and shear waves (V_L and V_S), Debye average velocity (V_m), melting point, Debye temperature (θ_D) and Grüneisen parameter (ζ) [40,41] have been calculated for $Rh_3(Zr,Hf)_xV_{1-x}$ ($x = 0$, 0.125, 0.25, 0.75, 0.875 and 1) compounds and are presented in table 2.

Debye temperature is one of the important parameter closely related to many physical properties such as elastic constants, specific heat, bond strength and melting temperature. It is used to measure the thermal conductivity of materials and also correlated to the strength of covalent bonds [42]. The Debye temperature, θ_D [43] and Grüneisen parameter, ζ [44] are two key quantities in solid-state problems due to their inherent relationship to lattice and molecular vibrations.
The following equations are used to calculate V_L, V_S, V_m [43] and Debye temperature (θ_D):

$$V_L = \sqrt{\frac{3B + 4G}{3\rho}},$$

$$V_S = \sqrt{\frac{G}{\rho}},$$

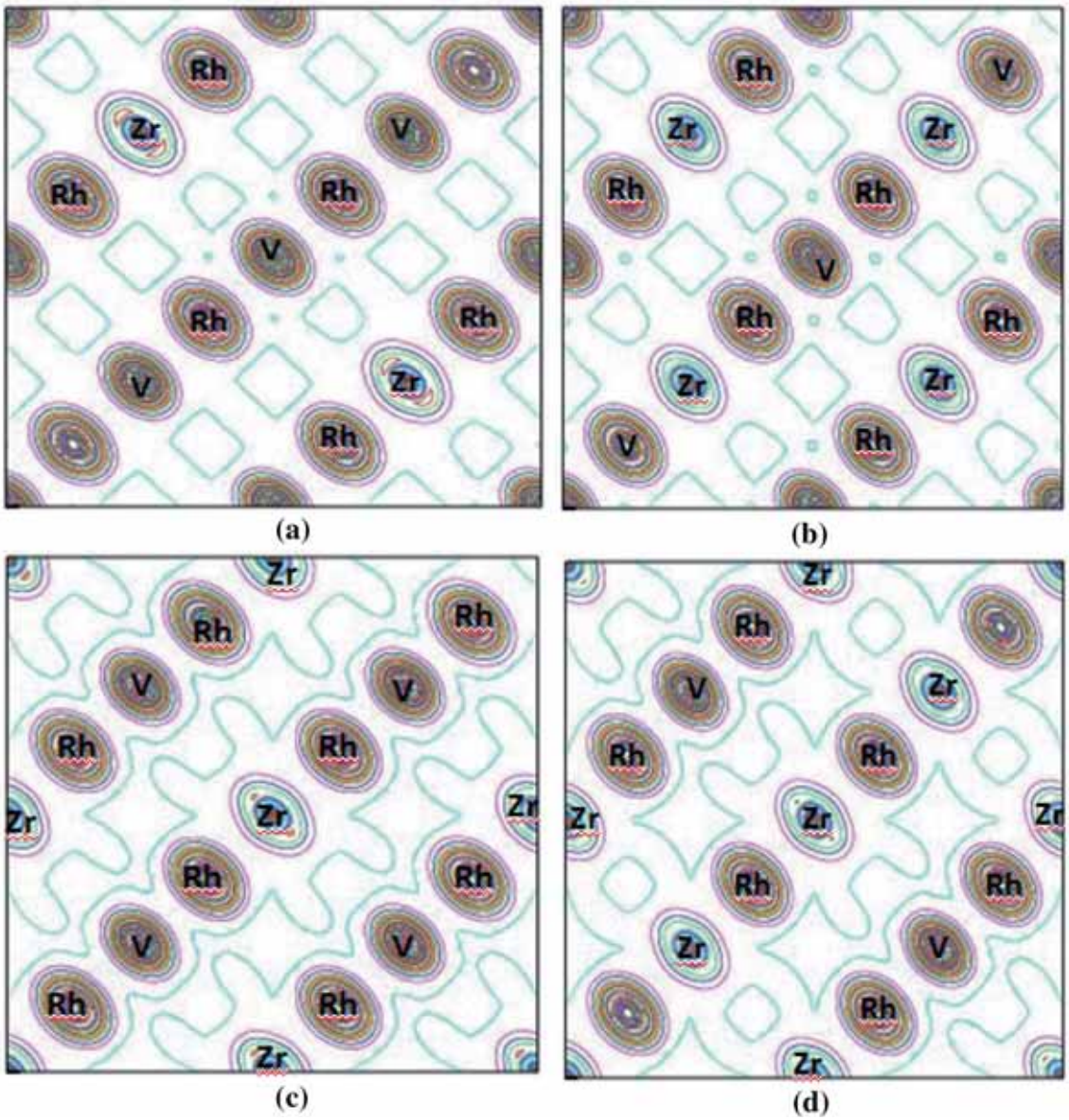

Figure 9. Charge density plot of (110) (**a**) $Rh_3Zr_{0.125}V_{0.875}$, (**b**) $Rh_3Zr_{0.25}V_{0.75}$, (**c**) $Rh_3Zr_{0.75}V_{0.25}$ and (**d**) $Rh_3Zr_{0.875}V_{0.125}$.

and

$$V_m = \left[\frac{1}{3}\left(\frac{1}{V_L^3} - \frac{2}{V_S^3}\right)\right]^{-1/3},$$

$$\theta_D = \left(\frac{\hbar}{k_B}\right)\left[\frac{3n}{4\pi V_a}\right]^{1/3} V_m.$$

The Debye temperature (θ_D) is directly related to average sound velocity (V_m), indicating greater the average sound velocity, the greater the Debye temperature. From table 2, it can be noted that in $Rh_3(Zr,Hf)_xV_{1-x}$ ($x = 0.125$, 0.25, 0.75 and 0.875) alloy combinations, the average sound velocities are found to be lesser for $Rh_3Zr_{0.25}V_{0.875}$ (3.5733 m s^{-1}) and $Rh_3Hf_{0.875}V_{0.125}$ (3.5291 m s^{-1}) combinations, respectively. Hence, the corresponding Debye temperature values are also lesser for $Rh_3Zr_{0.25}V_{0.875}$ (698 K) and $Rh_3Hf_{0.875}V_{0.125}$ (677 K) combinations. Therefore, in $Rh_3Zr_{0.25}V_{0.875}$ and $Rh_3Hf_{0.875}V_{0.125}$ combinations, the strength of covalent bond is weak, thereby leading to the possibility of more ductility in these compounds.

Grüneisen parameter (ζ) is the measure of anharmonicity of the crystal and it depends on elastic moduli through sound velocities. Harmonicity refers to a state where the lattice is associated with uniform lattice vibrations. Presence of large values of Grüneisen parameter for a given material indicates intense anharmonicity and/or soft bonding nature of the given

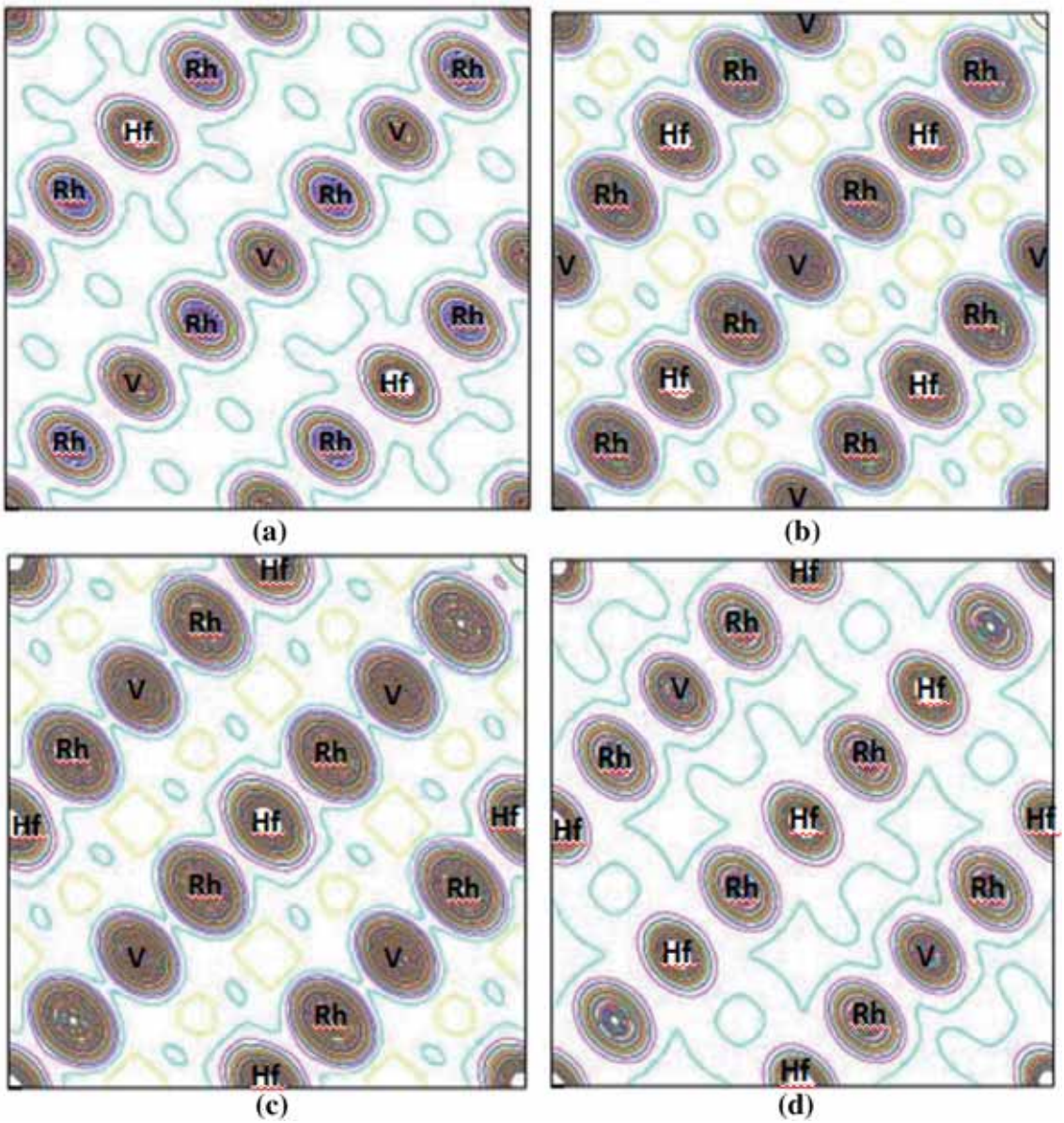

Figure 10. Charge density plot of (110) (**a**) $Rh_3Hf_{0.125}V_{0.875}$, (**b**) $Rh_3Hf_{0.25}V_{0.75}$, (**c**) $Rh_3Hf_{0.75}V_{0.25}$ and (**d**) $Rh_3Hf_{0.875}V_{0.125}$.

crystal. Here, Grüneisen parameter (ζ) is calculated using the expression given by,

$$\zeta = \frac{9\left(V_L^2 - \frac{4}{3}V_S^2\right)}{2\left(V_L^2 + 2V_S^2\right)},$$

where ($\hbar = h/2n$). h is the Plank constant, n the number of atoms per unit cell, V_a the volume of unit cell and k_B the Boltmann constant, respectively. From table 2, one can observe that in $Rh_3(Zr,Hf)_xV_{1-x}$ compounds, only for $Rh_3Zr_{0.25}V_{0.875}$ (1.7972) and $Rh_3Hf_{0.875}V_{0.125}$ (1.4886), the value of Grüneisen parameter is found to be large. Hence, the lower Debye temperature and larger Grüneisen parameter values indicate the weak covalent (soft) nature of $Rh_3Zr_{0.25}V_{0.875}$ and $Rh_3Hf_{0.875}V_{0.125}$ materials. The melting temperature (T_m) [20,21] of these alloys [45] are calculated using the following relation,

$$T_m = 553\ \text{K} + (5.91\ \text{K GPa}^{-1})C_{11} \pm 300\ \text{K}.$$

From table 2, one can find that the calculated melting temperature of Rh_3V, Rh_3Zr and Rh_3Hf materials are found to agree with the available experimental data as mentioned in the same table. The $Rh_3Zr_{0.25}V_{0.875}$ (2529 K) and $Rh_3Hf_{0.875}V_{0.125}$ (2353 K) combinations have the minimum value of melting

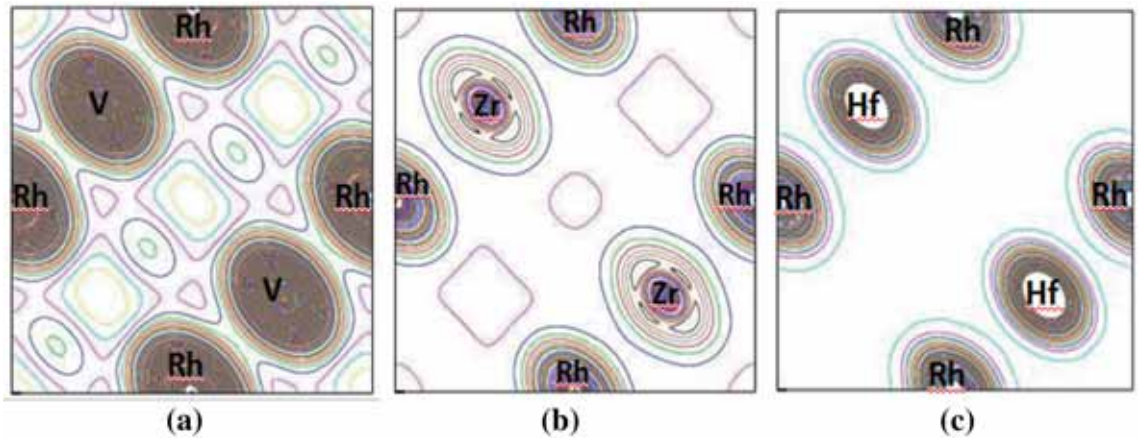

Figure 11. Charge density plot of (110) (**a**) Rh_3V, (**b**) Rh_3Zr and (**c**) Rh_3Hf.

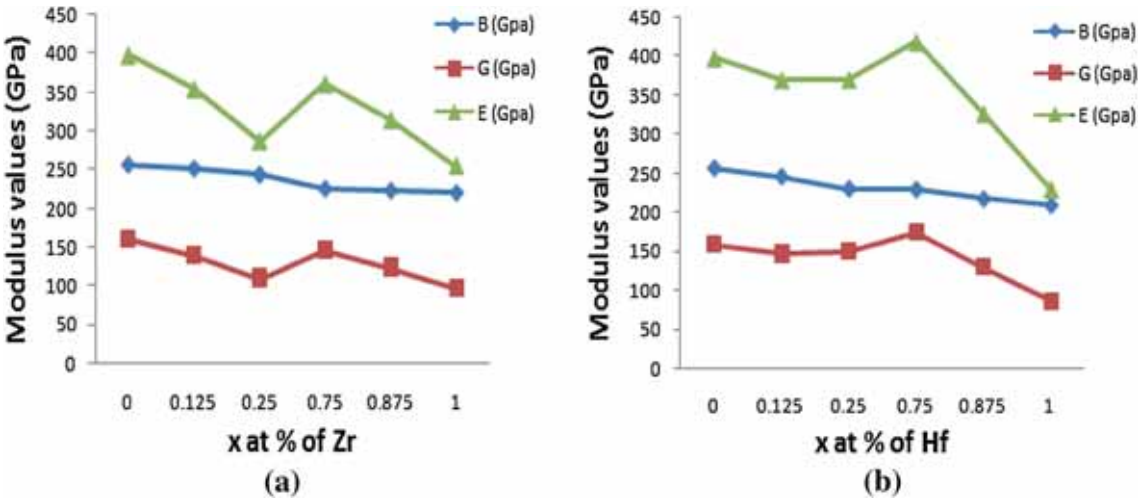

Figure 12. Modulus values *vs*. concentration of (**a**) $Rh_3Zr_xV_{1-x}$ and (**b**) $Rh_3Hf_xV_{1-x}$.

Table 2. Calculated volume, density (ρ), sound velocities for longitudinal and shear waves (V_L and V_S), Debye average velocity (V_m), Debye temperature (θ_D), melting temperature (T_m) and Grüneisen parameter (ζ) for $Rh_3(Zr,Hf)_xV_{1-x}$ ($x = 0$, 0.125, 0.25, 0.75, 0.875 and 1) alloys.

Alloy combinations	Volume (Å^3)	ρ (g cm^{-3})	V_L (10^3 m s^{-1})	V_S (10^3 m s^{-1})	V_m (10^3 m s^{-1})	θ_D (K)	T_m (K)	ζ
Rh_3V	55.343 55.089[a]	10.79 11.03[b]	6.8084	4.0981	4.5321	895	2788 2013[b]	1.3491
$Rh_3Zr_{0.125}V_{0.875}$	56.228	10.77	6.3735	3.6000	4.0042	786	2506	1.5787
$Rh_3Zr_{0.25}V_{0.75}$	57.078	10.75	6.0239	3.1975	3.5733	698	2298	1.7972
$Rh_3Zr_{0.75}V_{0.25}$	60.510	10.70	6.2688	3.6938	4.0933	784	2386	1.4267
$Rh_3Zr_{0.875}V_{0.125}$	61.153	10.72	6.0244	3.4029	3.7849	723	2305	1.5787
Rh_3Zr	61.950	10.71	5.7195	3.0151	3.3710	641	2281 2332[c]	1.8209
$Rh_3Hf_{0.125}V_{0.875}$	56.182	11.09	6.3200	3.6542	4.0563	797	2487	1.4949
$Rh_3Hf_{0.25}V_{0.75}$	56.937	11.42	6.2493	3.6287	4.0265	787	2420	1.4797
$Rh_3Hf_{0.75}V_{0.25}$	59.935	12.61	6.0573	3.7255	4.1111	790	2736	1.2701
$Rh_3Hf_{0.875}V_{0.125}$	60.405	12.95	5.4896	3.1797	3.5291	677	2353	1.4886
Rh_3Hf	62.055	13.04	4.9987	2.5846	2.8935	550	2389	1.8873

[a]Ref. [22], [b]ref. [3], [c]ref. [21].

temperature and the parent Rh_3V (2788 K) and $Rh_3Hf_{0.75}V_{0.25}$ (2736 K) compounds have the maximum value of melting temperature among the present materials under study.

4. Conclusion

The structural, electronic, mechanical and thermal properties of $Rh_3(Zr,Hf)_xV_{1-x}$ ($x = 0$, 0.125, 0.25, 0.75, 0.875 and 1) combinations are studied using the FP-LAPW method using DFT with GGA. The calculated lattice constants and bulk modulus are consistent with the literature values. From the band structure, the bands at the Fermi level originate from the interaction of Rh-d and hybridized d-states of V and Zr/Hf in $Rh_3(Zr,Hf)_xV_{1-x}$ ($x = 0.125$, 0.25, 0.75 and 0.875) combinations and the non-vanishing bands at the Fermi energy level show the metallic nature of the materials. From DOS histograms, the presence of deepest pseudogap in $Rh_3Zr_{0.75}V_{0.25}$, $Rh_3Hf_{0.75}V_{0.25}$ and $Rh_3Hf_{0.25}V_{0.75}$ combinations reflects the strength of covalent bonding (brittleness) of these materials. The directional electron density contours enclosing V–Rh–Zr–Rh atoms are observed in $Rh_3Zr_{0.75}V_{0.25}$ and $Rh_3Hf_{0.75}V_{0.25}$ combinations, reflecting their strong covalent nature; whereas in $Rh_3Hf_{0.125}V_{0.875}$ combination, comparatively weak directional contours reflects weak covalent nature and in $Rh_3Zr_{0.125}V_{0.875}$, $Rh_3Zr_{0.25}V_{0.75}$, $Rh_3Zr_{0.875}V_{0.125}$ and $Rh_3Hf_{0.875}V_{0.125}$ combinations, the absence of directional contours reflects their metallic nature. The calculated elastic constants display the elastically stable nature of newly predicted compounds of the present study.

The $Rh_3Zr_{0.25}V_{0.75}$ (286.63 and 109.91 GPa) and $Rh_3Hf_{0.875}V_{0.125}$ (326.69 and 130.93 GPa) combinations have the lowest and $Rh_3Zr_{0.75}V_{0.25}$ (360.33 and 145.99 GPa) and $Rh_3Hf_{0.75}V_{0.25}$ (418.57 and 175.02 GPa) combinations have the highest E and G values among the ternary $Rh_3Zr_xV_{(1-x)}$ and $Rh_3Zr_xV_{(1-x)}$ compounds under investigation. Out of these eight newly proposed alloy combinations, $Rh_3Zr_{0.25}V_{0.75}$ and $Rh_3Hf_{0.875}V_{0.125}$ compounds are identified as more ductile (less brittle) having the highest Cauchy pressure, Poisson's ratio and lowest G/B ratio, Shear modulus, Young's modulus and hardness values; whereas $Rh_3Zr_{0.75}V_{0.25}$ and $Rh_3Hf_{0.75}V_{0.25}$ combinations are identified as more brittle. The Debye temperature, Grüneisen parameter and melting temperature values are calculated for these compounds for the first time. The lower Debye temperature and larger Grüneisen parameter values indicate the weak covalent (soft) nature of $Rh_3Zr_{0.25}V_{0.875}$ and $Rh_3Hf_{0.875}V_{0.125}$ materials. The $Rh_3Zr_{0.25}V_{0.875}$ (2529 K) and $Rh_3Hf_{0.875}V_{0.125}$ (2353 K) combinations are observed to have the minimum value of melting temperature among the ternary compounds under study. The $Rh_3Hf_{0.75}V_{0.25}$ (2736 K) compound is predicted to have its melting temperature nearer to its parent binary Rh_3V (2788 K) compound.

Comparing the zirconium- and hafnium-doped ternary combinations of the present study with that of parent binary compound namely Rh_3V, the following $Rh_3Zr_{0.75}V_{0.25}$, $Rh_3Hf_{0.25}V_{0.75}$ and $Rh_3Hf_{0.75}V_{0.25}$ combinations are found to be more brittle, whereas the other ternary combinations namely $Rh_3Zr_{0.125}V_{0.875}$, $Rh_3Zr_{0.25}V_{0.75}$, $Rh_3Zr_{0.875}V_{0.125}$, $Rh_3Hf_{0.125}V_{0.875}$ and $Rh_3Hf_{0.875}V_{0.125}$ are found to be more ductile.

Acknowledgements

We wish to thank DRDO (ER & IPR), New Delhi, for the financial support through the project reference no. ERIP/ER/1203078/M/01/1507.

References

[1] Yamabe Mitarai Y, Koizumi Y, Murakami H, Ro Y, Maruko T and Harada H 1996 *Scr. Metall. Mater.* **35** 211
[2] Yamabe Mitarai Y, Ro Y and Murakami H 1998 *Metall. Mater. Trans. A* **29** 537
[3] Miura S, Honma K, Terada Y, Sanchez J M and Mohri T 2000 *Intermetallics* **8** 785
[4] Yamabe Mitarai Y, Ro Y, Maruko T and Murakami H 1998 *Scr. Mater.* **40** 109
[5] Yamabe Mitarai Y, Ro Y, Maruko T and Murakami H 1999 *Intermetallics* **7** 49
[6] Yamabe Mitarai Y, Nakazawa S and Harada H 2000 *Scr. Mater.* **43** 1059
[7] Fleischer R L 1987 *J. Mater. Sci.* **22** 2281
[8] Kim Y W 1989 *J. Met.* **41** 24
[9] Darolia R 1991 *J. Met.* **43** 44
[10] Dimiduk D M, Miracle D B, Kim Y W and Mendiratta M G 1991 *ISIJ Int.* **31** 1223
[11] Yoo M H, Sass S L, Fu C L, Mills M J, Dimiduk D M and George E P 1993 *Acta Metall. Mater.* **41** 987
[12] Liu C T, Stringer J, Mundy J N, Horton L L and Angelini P 1997 *Intermetallics* **5** 579
[13] Massalski T B (ed) 1990 In *Binary alloy phase diagram*, 2nd edn (Materials Park, OH: ASM International)
[14] Tetra Y, Ohkubo K, Miura S, Sanchez J M and Mohri T 2003 *J. Alloys Compd.* **354** 202
[15] Chen K, Zhao L R, Tse J S and Rodgers J R 2004 *Phys. Lett. A* **331** 400
[16] Kontsevoi Oleg Y, Gornostyrev Yuri N and Freeman Arthur J 2005 *JOM* **57** 43
[17] Rajagopalan M and Sundareswari M 2004 *J. Alloys Compd.* **379** 8
[18] Surucu G, Colakoglu K, Deligoz E and Ozisik H 2010 *Intermetallics* **18** 286
[19] Yamabe Mitarai Y, Koizumi Y, Murakami H, Ro Y, Maruko T and Harada H 1997 *Scr. Metall. Mater.* **36** 393
[20] Wang J J, Kuang X Y, Jin Y Y, Lu C and Huang X F 2014 *J. Alloys Compd.* **592** 42
[21] Ould Kada M, Seddik T, Sayede A, Khenata R, Bouhemadou A, Deligoz E *et al* 2014 *Int. J. Mod. Phys. B* **28** 145006
[22] Wang Tao-Fen, Chen Ping, Deng Yong-He and Tang Bi-Yu 2011 *Trans. Nonferrous Met. Soc. China* **21** 388
[23] Manjula M, Sundareswari M and Viswanathan E 2015 *Mater. Chem. Phys.* **108** 98

[24] Blaha P, Schwarz K, Madsen G K H, Kuasnicka D and Luitz J 2001 *WIEN2k: an augment plane wave plus local orbitals program for calculating crystal properties* (Wien, Austria: K Schwarz Technical University)
[25] Perdew J P, Chevary J A, Vosko S H, Jackson K A and Pederson M R 1992 *Phys. Rev. B* **46** 6671
[26] Perdew J P, Burke K and Ernzerhof M 1996 *Phys. Rev. Lett.* **77** 386
[27] Clark S J, Segall M D, Pickard C J, Hasnip P I, Probert M I J, Refson K *et al* 2005 *Kristallogr. Z* **220** 567
[28] Perdew J P and Zunger A 1981 *Phys. Rev. B* **23** 5048
[29] Birch F 1947 *Phys. Rev.* **71** 809
[30] Shi D, Wen B, Melnik R, Yao S and Li T 2009 *J. Solid State Chem.* **182** 2664
[31] Pettifor D 1992 *Mater. Sci. Technol.* **8** 345
[32] Pugh S F 1954 *Phil. Mag.* **45** 823
[33] Bannikov V V, Shein I R and Ivanovskii A L 2007 *Phys. Status Solidi RRL* **1** 89
[34] Deligoz E, Ozisik H, Colakoglu K, Surucu G and Ciftci Y O 2011 *J. Alloys Compd.* **509** 1711
[35] Milao N, Sa B, Zhou J and Sun Z 2011 *Comp. Mater. Sci.* **50** 1559
[36] Shein I R and Ivanovskii A L 2008 *J. Phys. Condens. Matter* **20** 415218
[37] Chandra Shekar N V and Sahu P Ch 2008 *Indian J. Phys.* **82** 1645
[38] Ozisik H, Deligoz E, Colakoglu K and Ateser E 2013 *Intermetallics* **39** 84
[39] Ranganathan S I and Ostoja Starzewski M 2008 *Phys. Rev. Lett.* **101** 055504
[40] Shein I R and Ivanovskii A L 2012 *Intermetallics* **26** 1
[41] Anderson O L 1963 *J. Phys. Chem. Solids* **24** 909
[42] Schreiber E, Anderson O L and Soga N 1973 *Elastic constants and their measurements* (New York: McGraw-Hill)
[43] Reddy P V, Reddy M B, Muley V N, Reddy K B and Ramana Y V 1988 *J. Mat. Sci. Lett.* **7** 1243
[44] Belomestnykh V N 2004 *Tech. Phys. Lett.* **302** 91
[45] Fine M E, Brown L D and Marcus H L 1984 *Scr. Metall.* **18** 951